



Application of remote sensing to identify coalfires in the Raniganj Coalbelt, India

Prasun K Gangopadhyay^{a,*}, Kuntala Lahiri-Dutt^b, Kanika Saha^c

^a *ESA Department, International Institute for Geo-Information Science and Earth Observation (ITC), Hengelostraat, P.O. Box 6, 7500 AA Enschede, The Netherlands*

^b *Resource Management in Asia Pacific Program, Research School of Pacific and Asian Studies, The Australian National University, Canberra, ACT 0200, Australia*

^c *Geography Department, Guskara Mahavidyala, Guskara, Burdwan, 713128 West Bengal, India*

Received 1 March 2005; accepted 19 September 2005

Abstract

Raniganj and Jharia regions together have been for long the single largest coal supplier in India, now contributing about a quarter of the total output in the country. Numerous reasons such as improper mining techniques and policy, as well as unauthorized mining caused surface and subsurface coalfires in these areas. These coalfires burn millions of tonnes of valuable coal resources, creating severe environmental problems and posing enormous operational difficulties of mining. After first use of remote sensing as a tool to identify coalfires in 1960s, with the time, the efficiency of remote sensing to identify and monitoring coalfires has been well established by several researchers. With the knowledge of local geological setting and density sliced surface temperature image the spatial distribution of coalfires can be revealed. The present paper makes an attempt to identify temperature anomalies of the Raniganj coalbelt to locate the spatial distribution of coalfires. Landsat Thematic Mapper (TM) thermal band data was used to calculate surface temperature along with NDVI (normalized vegetation index) derived emissivity.

© 2005 Elsevier B.V. All rights reserved.

Keywords: Coalfire; Remote sensing; Thermal infrared; Vegetation index

1. Introduction

Remote sensing has proven to be a reliable tool for studying earth surface and atmosphere in many applications. In case of high temperature object conditions, such as forest or mine fire, remote sensing can give a good synoptic view of the area under consideration. In the entire electromagnetic spectrum, 3–60 μm is considered as thermal infrared, whereas 3–5 and 8–12 μm is actually used in thermal remote sensing. Thermal-infrared sensing exploits the fact that

everything above absolute zero (-273°C) emits radiation in the thermal infrared range of the electromagnetic spectrum. Thermal infrared radiation of an object is controlled mainly by the characteristics of the surface: the emissivity, geometry of the object and its temperature.

Borehole temperature was the main tool to detect subsurface coalfires until the 1960s. The main advantage of this method was that temperature measurements can be done very close to fires but it was nearly impossible to gather enough data over a large area. In early 60's when airborne and later satellite borne data started to become available, the detection and monitoring of coalfires become easier. Studies in the United States, Australia, India and China were done by different researchers using remote sensing as a prime tool.

* Corresponding author. Fax: +31 53 487 4336.

E-mail addresses: prasun@itc.nl (P.K. Gangopadhyay), kuntala@coombs.anu.edu.au (K. Lahiri-Dutt), kanika_saha@yahoo.com (K. Saha).

As most coal producing countries, the United States also has a serious coalfire problem. Using the 'Reconofax' thermal scanner on an airborne platform, Slavecki (1964), Knuth (1968) and Greene et al. (1969) studied fires on waste coal and subsurface coalfires in Pennsylvania.

In Australia, among the natural coalfires, the burning mountain in New South Wales is a well-known coalfire, which was discovered in 1828. Later Ellyett and Fleming (1974) estimated the age of the fire to be at least 6000 years.

In India, the Jharia coalfield, which is 250 km northwest from Kolkata (Calcutta), has severe problems of coalfire. Cracknell and Mansor (1992) first used Landsat-5 TM and NOAA-9 AVHRR data and found that night time NOAA data was quite useful to isolate the warm areas from the background. Reddy et al. (1993) used the short-wave infrared (SWIR) region of the EMR, which is covered by Landsat TM band 4, 5 and 7. Later Prakash et al. (1997) used the Landsat TM TIR and SWIR bands to identify surface and subsurface fires separately.

With an enormous resource of coal, coalfire is also an immense problem in northern China. In Xinjiang and Ningxia Hui regions, several ITC (Enschede, Netherlands) researchers worked on coalfire. By using pre-dawn airborne thermal scanner data, Yang (1995) identified several coalfires in these areas, which correlated well with field observations. Later Wan and Zhang (1996) and Zhang et al. (1997, 1998) carried out a detailed study in the same area. In 1996, Genderen et al. developed a method to synergistic use of remote sensing data to detect underground coalfire. By analyzing SWIR spectra of rocks, Zhang (1996) could identify the burnt rocks, which is also an indication of coalfire.

Subsequently, an attempt was made to model coalfire scenarios to understand the phenomenon more effectively. This involved estimating the spread of fire using different sensors and development of a dedicated remote sensing/GIS coalfire detection monitoring system for decision making (Rosema et al., 2001; Prakash and Vekerdy, 2004; Zhang et al., 2004; Voigt et al., 2004).

Most of the aforesaid studies related to surface temperature extraction to identify coalfires from remote sensing data, were based on certain fixed emissivity value (0.95). The main reason behind this limitation was that it is not possible to obtain temperature and emissivity from passive radiometry separately because the number of unknowns is always larger than the number of measurements (Becker, 1980). But the knowledge of land surface emissivity is necessary to

extract more reliable temperature from (a certain) thermal infrared data. Using a single thermal band it is impossible to get such information from the available methods such as temperature emissivity separation algorithm (TES) (Gillespie et al., 1998). TES method, based on ASTER data, returns a reliable land surface emissivity of an area under investigation (Gangopadhyay, 2003; Gangopadhyay et al., in press). In the case of single band thermal data a possible option to extract land surface emissivity could be a classified image, in which an emissivity value for each class is assumed. However, without a very detailed knowledge of different classes of study area and a realtime (ground) data it will not be very functional (Dash et al., 2005). Another functional option could be to extract land surface emissivity from NDVI that has described by many researchers (van de Griend and Owe, 1993; Valor and Caselles, 1996; Sobrino and Raissouni, 2000; Sobrino et al., 2004). The method proposed obtains the emissivity values from the NDVI considering three different cases:

- (a) $NDVI < 0.2$: pixels with NDVI values less than 0.2 are considered as bare soil,
- (b) $NDVI > 0.5$: in this case, the pixel is considered as mostly vegetated, and
- (c) $0.2 < NDVI < 0.5$: in this case, the pixel is composed by a mixture of bare soil and vegetation, and the emissivity can be calculated using the equations described by Valor and Caselles (1996). The detailed methodology is described in Section 3 (Methodology).

Despite the fact satellite remote sensing has established as a significant tool in the field of coalfire detection and monitoring, few constraints have not been overcome. In most cases, coalfire is a very local phenomenon and not large enough to saturate a whole pixel to appear as an anomaly in comparison to the background. The aggregated temperature of a pixel depends on the location, spread, surface type and temperature of the fire/crack and it's surrounding. With a spatial resolution of 120 m, Landsat5 TM6 is big enough to accommodate few cracks with active fire, local rocks and (sometimes) sparse vegetation. These different kinds of landcovers may have different temperature ranges to influence each other and finally appear as an anomaly or background with a certain pixel integrated temperature value. Though a comparatively higher resolution data (ASTER, ETM+), can return more reliable surface temperature because of more chance of homogenous pixel, the present research

attempts to extract surface temperature anomalies related to coalfires on experimental basis using NDVI derived emissivity. This paper discusses a case study in eastern India where coalfire related anomalies were extracted qualitatively using Landsat-5 thermal data.

2. Study area

The Raniganj coalbelt (Fig. 1) comprises a total area of nearly 1260 km², and is located about 250 km northwest of Kolkata, the capital of West Bengal, an eastern state of India. The area is bounded by 23°33' and 23°53'N latitude and 86°37' and 87°23'E longitude. A major part of the Raniganj coalfield according to the Coal India Limited definition falls within Burdwan district (of West Bengal), which we have identified as our study area.

The sedimentary rock formations which comprise Raniganj coalbelt – excluding the recent and subrecent alluvial and lateritic deposits – all belong to Gondwana system which extended over a considerable portion of the southern hemisphere (Gee, 1932). Permocarboiferous rock formations of Talcher, Barakar, Barren measures, Raniganj and Panchet series are exposed in many places. The southern boundary is represented by a

well defined fault of an immense down throw to the north (Blanford, 1861). According to a recent Geological Survey of India (GSI) report, Raniganj coalbelt has second largest resource of coal (25 billion tonnes) in India (<http://www.gsi.gov.in/indiacoal.pdf>).

3. Methodology

Landsat 5 Thematic Mapper (TM) bands 3, 4 and 6 acquired on 30 April 1997 (daytime) were used for the study. To identify the thermal anomalies related to coalfires, satellite and ground (or field) measurements are used. The aim of surface or ground data collection is to obtain information about geographic features and phenomena through in situ measurements to validate processed satellite data. The five major components of ground data collection are: (a) temperature, (b) geographical position, (c) attribute or surface properties, (d) spatial relationship and (e) satellite overpass time.

3.1. Pre-processing of Landsat TM data

To reduce the atmospheric effect of Landsat TM3 and TM4 data ATCOR2 (Richter, 2005) was used. As the area is characterized by a very gently undulating

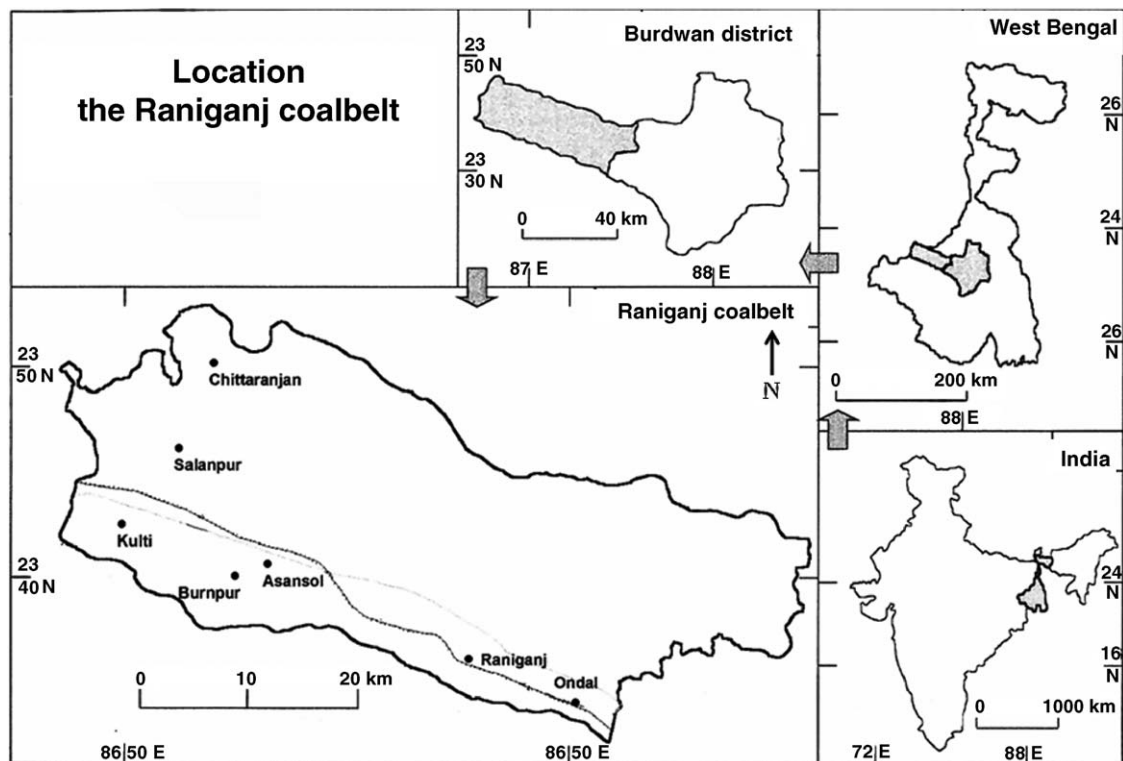


Fig. 1. The study area, Raniganj Coalbelt, India.

topography with average height of the ground level varying between 73 and 120 m, it was expected solar heating does not have much role to produce false anomalies. However, these atmospherically corrected images were used for further processing.

3.2. Processing of TM data

The atmospherically corrected red and infrared bands were later used for NDVI calculation to extract surface emissivity. Thermal infrared band or TM6 of Landsat was used to extract brightness temperature by using the method described below.

The digital values of thermal band were converted to spectral radiance using the following equation (Markham and Barker, 1986)

$$L_{\lambda} = L_{\min(\lambda)} + \frac{L_{\max(\lambda)} - L_{\min(\lambda)}}{Q_{\text{cal max}}} Q_{\text{cal}} \quad (1)$$

where L_{λ} is the spectral radiance; $L_{\min(\lambda)}$ the minimum detected spectral radiance for the scene ($0.1238 \text{ mw cm}^{-2} \text{ Sr}^{-1} \mu\text{m}^{-1}$); $L_{\max(\lambda)}$ the maximum detected spectral radiance for the scene ($1.56 \text{ mw cm}^{-2} \text{ Sr}^{-1} \mu\text{m}^{-1}$); Q_{cal} the grey level for analysed pixel; $Q_{\text{cal max}(\lambda)}$ the maximum grey level.

Once the spectral radiance (L_{λ}) for TM band 6 is computed, it is possible to calculate radiant temperature directly by the following equation:

$$T_{\text{R}} = \frac{K_2}{\ln((K_1/L_{\lambda}) + 1)} \quad (2)$$

where T_{R} is the radiant temperature (K); L_{λ} the spectral radiance ($\text{mw cm}^{-2} \text{ srt}^{-1} \mu\text{m}^{-1}$); K_1 the calibration constant ($60.776 \text{ mw cm}^{-2} \text{ Sr}^{-1} \mu\text{m}^{-1}$); K_2 the calibration constant (1260.56 K).

To enhance the vegetation characteristics over an area under consideration, the vegetation index is widely used in many applications. One of the most common vegetation indices is NDVI, which can be calculated as

$$\text{NDVI} = \frac{(\rho_2 - \rho_1)}{(\rho_2 + \rho_1)} \quad (3)$$

where ρ_2 is the spectral reflectance measured in NIR band (TM 4); ρ_1 the spectral reflectance measured in red band (TM 3). To calculate the emissivity it is necessary to calculate NDVI of a mixed pixel. Considering a mixed pixel of TM6 in which vegetation has occupied an area P_{v} and soil occupied $(1 - P_{\text{v}})$ (Fig. 2), the NDVI becomes (Valor and Caselles, 1996)

$$i = i_{\text{v}}P_{\text{v}} + i_{\text{g}}(1 - P_{\text{v}}) \quad (4)$$

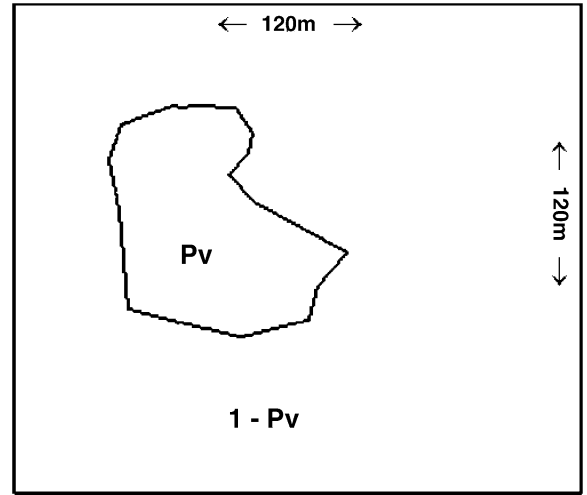


Fig. 2. A mixed pixel of TM6 in which vegetation has occupied an area P_{v} and soil occupied $(1 - P_{\text{v}})$.

where i is the NDVI value of the mixed pixel, and i_{v} and i_{g} are the values of the vegetation and ground.

The value of i (NDVI of a mixed pixel) is calculated through the satellite data using the following equation:

$$P_{\text{v}} = \frac{1 - (i/i_{\text{g}})}{(1 - (i/i_{\text{g}})) - \kappa(1 - (i/i_{\text{v}}))} \quad (5)$$

where i is the NDVI value of mixed pixel; i_{v} is the NDVI value of pure vegetation; i_{g} is the NDVI value of pure soil and

$$\kappa = \frac{\rho_{2\text{v}} - \rho_{1\text{v}}}{\rho_{2\text{g}} - \rho_{1\text{g}}} \quad (6)$$

where $\rho_{1\text{v}}$ and $\rho_{2\text{v}}$ are reflectance values of vegetation in red and NIR; $\rho_{1\text{g}}$ and $\rho_{2\text{g}}$ are reflectance values of soil in red and NIR.

The emissivity values were calculated using the following equation (van de Griend and Owe, 1993):

$$\varepsilon = a + b \ln(i) \quad (7)$$

With a correlation coefficient of 0.941 with $a = 1.0094$ and $b = 0.047$ at a 0.01 level of significance.

From the radiant temperature T_{R} can be converted into kinetic temperature (T_{K}) using

$$T_{\text{R}} = \varepsilon^{1/4} T_{\text{K}} \quad (8)$$

where T_{R} is the radiant temperature (K); ε the spectral emissivity; T_{K} the kinetic temperature (K).

The digital values Landsat-5, TM6 have been converted into kinetic temperature using the above equations. Then applying suitable corrections, land surface temperature mapping has been done and the locations of the mine fires were identified.

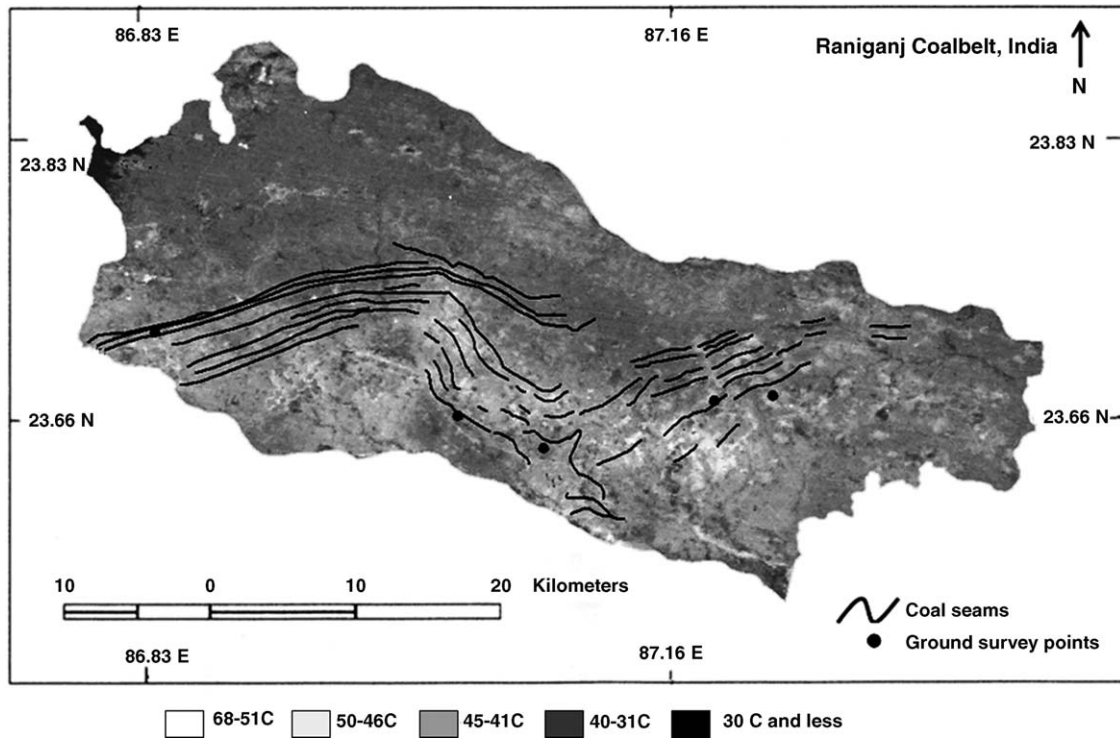


Fig. 3. Density sliced surface temperature map with high temperature anomalous areas.

The isothermal zonation on the basis of temperature gradient has been done. The temperature of different landcover types was found to be in close agreement with the ground realities as observed in the field and satellite data.

3.3. Field based methods

To estimate the temperature of different surfaces and crack/fires a handheld Raytek radiant thermometer was used. This instrument operates in a wide region of temperature (-32 to 760 °C), spectral coverage (8 – 14 μm) and the emissivity can be defined with a precision of 0.01 . A laser pointer makes it easy to point on a particular object from a distance. Most measurements were recorded along the cracks from a typical distance of ~ 1 m except for some inaccessible areas. In those cases the measurements were recorded from a distance of ~ 5 m. With an accuracy of ± 1 °C (in the range of 23 – 760 °C) it was the best available instrument during fieldwork. It should be noted that the Raytek instrument has an operating window of 8 – 14 μm , whereas band TM6 is located in the range of 10.40 – 12.50 μm . Due to this difference in operating region of EMR, some errors are expected.



Fig. 4. Smoke is coming out from a crack from a shallow coalfire on the surface that is partially subsided.

4. Results and discussions

Landsat TM recorded on 30 April 1997 of Raniganj coalbelt and surrounding area was used for the present study. In raw data itself, there was a good contrast between suspected coalfire area and the surroundings. After processing the thermal data, some point measurements were done in a nearby water reservoir (located north-west of study area) which has relatively homogenous pixels, for validation purpose. The surface temperature and density sliced image (Fig. 3) of the study area displays the different zone of temperatures. The density sliced image shows five temperature zones, four of them are in different grey tones that represents 68–51, 50–46, 45–41, 40–30, 29–15 °C, respectively. The bright white patches near Raniganj (Figs. 1 and 3) show high temperature events due to surface and subsurface coalfires. The total area can be grouped into five categories (based on ground observations):

1. areas of prominent temperature anomalies, coloured in white,
2. areas of heat flow from those anomalies and habitation, coloured in light grey,
3. surrounding areas, coloured in medium grey,
4. vegetated/agricultural land, coloured in dark grey, and
5. water bodies, swamps, coloured in black.

3. surrounding areas, coloured in medium grey,
4. vegetated/agricultural land, coloured in dark grey, and
5. water bodies, swamps, coloured in black.

Over water surface the temperature was found to be 12–22 °C whereas the temperature over vegetation was found to be in the range of 21–26 °C including agricultural and dense vegetation cover. This is because vegetation tries to attain equilibrium with the air temperature (Metzier and Malila, 1985). The temperatures of barren and fallow lands with sparse vegetation were found in the range between 29 and 38 °C, but in some absolutely open bare soil and coal spoil dumps displays higher temperature (+40 °C). Over the settlements the temperatures were found in the range of 28–34 °C. The temperatures on the overburden dumps of the open cast mines were found to be between 28 and 32 °C and inside the mine between 35 and 38 °C. The maximum temperature was observed over the coal seams, which extends from east to west. The temperatures over the coal seams at some places are more than 50 °C. In some places the temperature was found to be as high as 68 °C (Fig. 4).

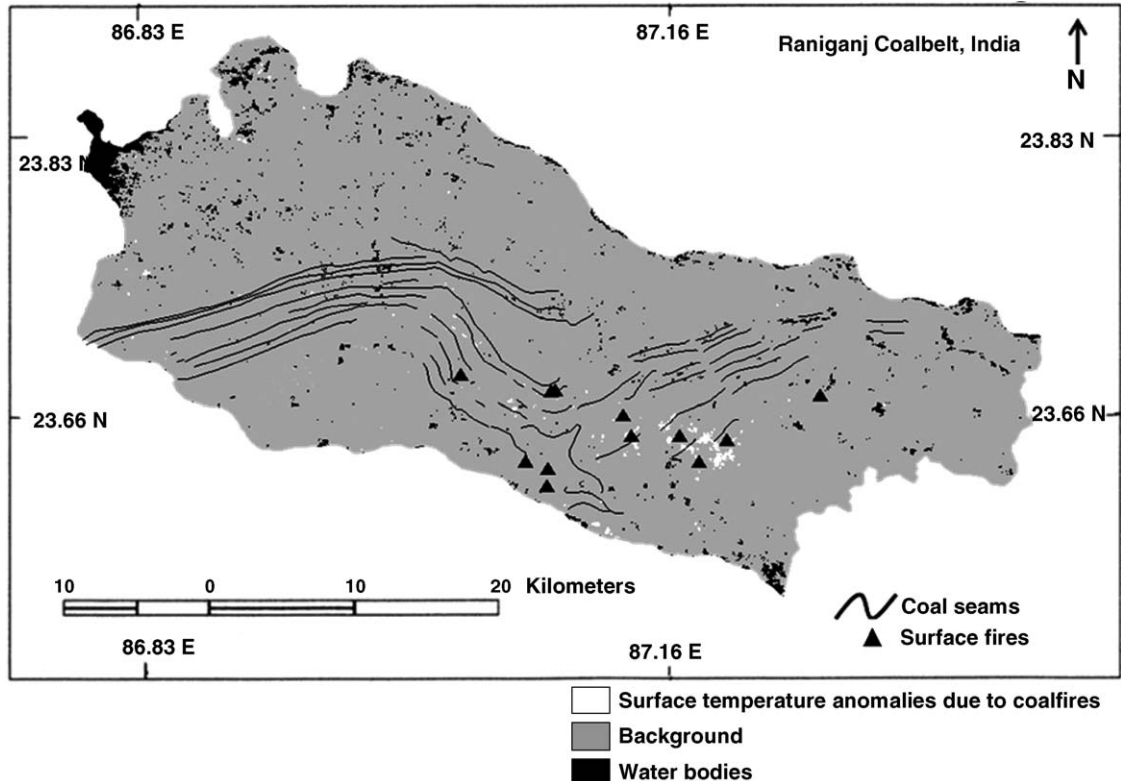


Fig. 5. Location of surface coalfires in relation to local geological settings and ground knowledge.

It is known that TM6 saturates at 68 °C (Rothery et al., 1998). In this study the pixels with saturation temperature are assumed to be the surface coalfire. The possible other hotspots such as chimney of factories were identified during the ground truth survey and with help of Survey of India topographical sheets. Those were eliminated from further processing. The final surface temperature map shows the surface coalfire affected areas (Fig. 5) in relation to local geological setting and ground information.

Emissivity is not only a factor affecting the accuracy of satellite temperature data, but also depends on the local atmospheric condition. However, in the present research, the thermal channel data was used without any atmospheric correction because during primary validation it was found the temperature difference between processed data and ground truth is very close (± 2 °C) in a homogeneous area like water reservoir.

5. Conclusions

Since 1960s remote sensing has been used as a reliable tool for coalfire detection and monitoring. The present study shows that Landsat-5 thermal remote sensing image can reveal the surface temperature anomalies effectively for quantitative study of coalfire. But in some cases, inaccurate pixel integrated temperatures are expected because of mixing of high temperature events (coalfires) and background, which is a major drawback of low resolution data. Furthermore, a good knowledge of local geology can interpret and differentiate the coalfire induced anomalies more accurately from some low thermal inertia rocks which can appear as a false anomaly due to fast solar heating. The results also shows use of NDVI derived emissivity can return a more reliable surface temperature rather than use of a fixed emissivity for all types of landcover. However, it should be noted that vegetation type, water content of leaf and view angle can influence the expected result. Though in a mining area like Raniganj coalbelt where average height is between 73 and 120 m, solar heating does not play an important role to produce false anomalies, still some overburden dumps of opencast mines with low thermal inertia rocks and coaldust can appear as false anomalies. To eliminate solar heating related false anomalies DEM correction (Dymond and Shepherd, 1999) is a well established method. But in a very active mining area like Raniganj, where topography changes rapidly with mining activity, DEM correction is not feasible because of non-availability of terrain model during time of satellite acquisition.

Acknowledgements

The authors would like to thank Dr. P.S. Roy, NRSA, India, Dr. A. Prakash UAF, GI, USA Professor J.L. van Genderen and Dr. P. van Dijk, ITC, The Netherlands, for their contributions in this study. Also, the authors also duly acknowledge the critical comments from reviewers that have helped to improve this paper.

References

- Becker, F., 1980. In: Frayse, G. (Ed.), Remote Sensing Applications in Agriculture and Hydrology. Balkema.
- Blanford, W.M., 1861. On the geological structures and relation of the Raniganj coalfield, Bengal. *Memoirs of the Geographical Survey of India*, vol. 8, Part I. .
- Cracknell, A.P., Mansor, S.B., 1992. Detection off sub-surface coal fires using Landsat Thematic Mapper data. *Int. Arch. Photogr. Rem. Sens.* 29 (b7), 750–753.
- Dash, P., Gfittsche, F.-M., Olesen, F.-S., Fischer, H., 2005. Separating surface emissivity and temperature using two-channel spectral indices and emissivity composites and comparison with a vegetation fraction method. *Rem. Sens. Environ.* 96, 1–17.
- Dymond, J.R., Shepherd, J.D., 1999. Correction of the topographic effect in remote sensing. *IEEE Trans. Geosci. Rem. Sens.* 37, 2618–2620.
- Ellyett, C.D., Fleming, A.W., 1974. Thermal infrared imagery of the burning mountain coalfire. *Rem. Sens. Environ.* 3, 79–86.
- Gangopadhyay, P.K., 2003. Coalfire detection and monitoring in Northern China: A multi-spectral and multi-sensor TIR approach. M.Sc. Thesis, ITC, Enschede, The Netherlands.
- Gangopadhyay, P.K., Maathuis, B., van dijk, P., in press. ASTER derived emissivity and coalfire related surface temperature anomaly: a case study in Wuda, North China. *Int. J. Rem. Sens.*
- Gee, E.R., 1932. *Memoirs of the Geological Survey of India, The geology and coal resources of the Raniganj Coalfield, Part I* (Gee, I.B.).
- Gillespie, A.R., Rokugawa, S., Hook, S., Matsunaga, T., Kahle, A.B., 1998. A temperature and emissivity separation algorithm for advanced spaceborne thermal emission and reflection radiometer (ASTER) images. *IEEE Trans. Geosci. Rem. Sens.* 36, 1113–1126.
- Greene, G.W., Moxham, R.M., Harvey, A.H., 1969. Aerial infrared surveys and borehole temperature measurements of coal mine fires in Pennsylvania. In: *Proceedings of the Sixth International ERIM Symposium on Remote Sensing Environment*, University of Michigan, USA, 13–16 October, pp. 517–525.
- Knuth, W.M., 1968. Using an airborne infrared imaging system to locate subsurface coal fires, in *Culm banks*. *Proc. Pennsylvania Acad. Sci. U.S.A.* 42.
- Markham, B.L., Barker, J.L., 1986. Landsat MSS and TM post calibration dynamic ranges, exoatmospheric reflectance and at-satellite temperatures. *EOSAT Landsat Technical Notes 1*. Earth Observation Satellite Co., Lanham, Maryland, EOSAT, USA, pp. 3–8.
- Metzier, M.C., Malila, W.A., 1985. Characterization and comparison of Landsat 4 and Landsat 5 Thematic Mapper data. *Photogr. Eng. Rem. Sens.* 15, 1315–1330.

- Prakash, A., Vekerdy, Z., 2004. Design and implementation of a dedicated prototype GIS for coal fire investigations in North China. *Coal Geol.* 59, 107–119.
- Prakash, A., Gupta, R.P., Saraf, A.K., 1997. A Landsat TM based comparative study of surface and subsurface fires in the Jharia coalfield. *India Int. J. Rem. Sens.* 18 (11), 2463–2469.
- Reddy, C.S.S., Srivastav, S.K., Bhattacharya, A., 1993. Application of Thematic Mapper short wavelength infrared data for the detection and monitoring of high temperature related geoenvironmental features. *Int. J. Rem. Sens.* 14, 3125–3132.
- Richter, R., 2005. Atmospheric/topographic correction for satellite imagery (ATCOR 2/3 User Guide, Version 6.1, January 2005), DLR, Remote Sensing Center, Wessling. DLR-IB 565-01/05, Germany, p. 57.
- Rosema, A., Guan, H., Veld, H., 2001. Simulation of spontaneous combustion, to study the causes of coal fires in the Rujigou Basin. *Fuel* 80, 7–16.
- Rothery, D.A., Francis, P.W., Wood, C.A., 1998. Volcano monitoring using short wavelength infrared data from satellite. *J. Geophys. Res.* 93, 7993–8008.
- Slavecki, R.K., 1964. Detection and location of subsurface coal fires. In: *Proceedings of the Third Symposium on Remote Sensing and Environment*, Ann Arbor, University of Michigan, Michigan, USA, pp. 537–547.
- Sobrino, J.A., Raissouni, N., 2000. Towards remote sensing methods for land cover dynamic monitoring, application to Morocco. *Int. J. Rem. Sens.* 21, 353–366.
- Sobrino, J.A., Jimenez-Munoz, J.C., Paolini, L., 2004. Land surface temperature retrieval from LANDSAT TM 5. *Rem. Sens. Environ.* 90, 434–440.
- Valor, E., Caselles, V., 1996. Mapping land surface emissivity from NDVI: application to European, African and South American areas. *Rem. Sens. Environ* 57, 167–184.
- van de Griend, A.A., Owe, M., 1993. On the relationship between thermal emissivity and the normalized difference vegetation index for natural surfaces. *Int. J. Rem. Sens.* 14 (6), 1119–1131.
- Voigt, S., Tetzlaff, A., Zhang, J., Künzer, C., Zhukov, B., Strunz, G., Oertel, D., Roth, A., Van Dijk, P.M., Mehl, H., 2004. Integrating satellite remote sensing techniques for detection and analysis of uncontrolled coal seam fires in North China. *Int. J. Coal Geol.* 59 (1–2), 121–136.
- Wan, Y.Q., Zhang, X.M., 1996. Using a DEM to reduce the effect of solar heating on Landsat TM thermal IR images and detection of coalfires. *Asia-Pacific Rem. Sens. GIS J.* 8, 65–72.
- Yang, H., 1995. Detection of areas of spontaneous combustion of coal using airborne and TM data in Xinxiang, China. M.Sc. Thesis, ITC, Enschede, The Netherlands.
- Zhang, X.M., Cassells, C.J.S., van Genderen, J.L., 1998. Multispectral data fusion for the detection of underground coalfires. *Geol. Mijnb.* 77, 117–127.
- Zhang, X.M., van Genderen, J.L., Kroonenberg, S.B., 1997. A method to evaluate the capability of Landsat-5 TM band 6 data for sub-pixel coalfire detection. *Int. J. Rem. Sens.* 18 (15), 3279–3288.
- Zhang, J., Wagner, W., Prakash, A., Mehl, H., Voigt, S., 2004. Detecting coal fires using remote sensing techniques. *Int. J. Rem. Sens.* 25 (16), 3193–3220.
- Zhang, J.Z., 1996. SWIR spectra of rocks in areas affected by coalfires, Xinjinag autonomous region PR China, MSc Thesis, ITC, Enschede, The Netherlands.